To appear in the *Journal of Geophysical Research*, 1998.

Deconvolution of interplanetary transport of solar energetic particles

D. Ruffolo, T. Khumlumlert,[1] and W. Youngdee

Department of Physics, Chulalongkorn University, Bangkok, Thailand

arXiv:astro-ph/9806097v1 6 Jun 1998

Abstract

We address the problem of deconvolving the effects of interplanetary transport on observed intensity and anisotropy profiles of solar energetic particles with the goal of determining the time profile and spectrum of particle injection near the Sun as well as the interplanetary scattering mean free path. Semi-automated techniques have been developed to quantitatively determine the best fit injection profile, assuming (1) a general piecewise linear profile or (2) a Reid profile of the form $[C/(t-t_0)]\exp[-A/(t-t_0)-(t-t_0)/B]$. The two assumptions for the form of the injection profile yielded similar results when we tested the techniques using ISEE 3 proton data from the solar flare events of July 20, 1981 (gradual flare), and January 2, 1982 (impulsive flare). For the former event, the duration of injection was much shorter for protons of higher energy (75-147 MeV), which may be interpreted as indicating that the coronal mass ejection-driven shock lost the ability to accelerate protons to $\sim$100 MeV after traveling beyond a certain distance from the Sun.

1. Introduction

One of the basic questions one can ask about energetic particles produced by solar activity is how many are accelerated as a function of energy and time. Electromagnetic and neutron diagnostics of interacting energetic particles can provide a wealth of information on the particle spectrum and the timing of particle acceleration at the flare site [e.g., *Chupp,* 1990; *Aschwanden et al.,* 1994; *Aschwanden,* 1996; *Debrunner et al.,* 1997; *Rank et al.,* 1997a, b]. Complementary information can be obtained from spacecraft or ground-based observations of escaping, energetic, charged particles. The interpretation of these direct observations is complicated by the effects of interplanetary transport, particularly scattering due to irregularities in the interplanetary magnetic field [*Meyer et al.,* 1956]. To date, such observations have always been performed at distances approximately 0.3 AU or greater from the Sun, while the mean-free path of interplanetary scattering parallel to the magnetic field, $\lambda_{\|}$, is typically between 0.08 and 0.3 AU (near the Earth), though it can be $>$ 1AU for infrequent "scatter-free" events [*Palmer,* 1982]. Since the distance from the Sun to the observer is of the same order of magnitude as, and usually larger than, the mean-free path, the interplanetary transport is largely diffusive in most cases, making it difficult to determine the underlying time profile of injection near the Sun and possibly affecting the measurement of the spectrum.

Why should we go through the trouble of deconvolving the effects of interplanetary transport to determine the injection profile of escaping energetic particles, when electromagnetic or neutron diagnostics of interacting particles can yield such information more directly? A key motivation is that it has recently become widely accepted that for many flare events the interacting and escaping energetic particles are accelerated in different locations and possibly by different mechanisms. Twenty years ago, it was recognized from X ray observations that solar flares can be basically classified into two groups [*Pallavicini et al.,* 1977], which are now commonly called "impulsive" and "gradual" according to the duration of their X ray emission. More recently, flares in these two categories have been found to exhibit many other differences in their physical properties and particle emissions, although measurements of ionic charge states indicated that ions from both types of flares are accelerated out of coronal material [*Luhn et al.,* 1984, 1987]. One key difference is that gradual flares are much more likely to be associated with coronal mass ejections (CMEs), which in turn often drive a traveling interplanetary shock [*Sheeley et al.,* 1983]. For over a decade there has been mounting circumstantial evidence that for flare/CME events, the flare is responsible for accelerating interacting particles, while the CME and/or associated shock is responsible for accelerating escaping ions on open magnetic field lines over a wide range of heliolongitudes [e.g., *Mason et al.,* 1984; *Lee and Ryan,* 1986; *Reames,* 1990]. (The origin of escaping electrons is subject to debate, but there is some evidence that they come from the flare site [*Dröge et al.,* 1990a].) Further evidence against the alternative and previously accepted view that escaping ions are accelerated at the flare site followed by transport within the corona is provided by recent Solar, Anomalous, and Magnetospheric Particle Explorer (SAMPEX) measurements of the charge states of escaping ions [*Leske et al.,* 1995; *Mason et al.,* 1995; *Oetliker et al.,* 1997], which rule out transport within the corona for longer than $\sim$1 min [*Ruffolo,* 1997]. Therefore observations of escaping ions can provide unique information about the acceleration of ions out of coronal material in the CME/shock region [*Kahler et al.,* 1990].

For impulsive flare events, the remarkable enhancement of the ^{3}He/^{4}He ratio among escaping ions [*Hsieh and Simpson,* 1970] by up to a factor of thousands is best explained by turbulent acceleration in the flare region [*Fisk,* 1978]. The observed longitudinal distribution of solar energetic particles from impulsive events (albeit narrower than for gradual events) could be explained by interplanetary transport perpendicular to the average magnetic field or by transport within the corona. Thus, for impulsive events, a deconvolution of the effects of interplanetary transport along the field could be useful for characterizing the process of azimuthal transport, especially if one studies data from multiple spacecraft at different locations.

Previous analyses of the intensity and/or anisotropy of solar energetic particles versus energy and time for various solar flare/CME events have yielded information on (1) the injection of particles near the Sun versus energy and time and (2) the mean-free path of interplanetary scattering. In most cases, both must be determined to provide a good fit to the data, although some previous studies have reported adequate fits by assuming an instantaneous injection of particles for some events.

Previous fits to solar energetic particle observations have employed various assumptions about in-

terplanetary transport. Some authors have restricted their analyses to cases where the mean-free path is believed to be long and have neglected interplanetary transport effects altogether [e.g., *Debrunner et al.,* 1988; *Kahler et al.,* 1990; *Kallenrode and Wibberenz,* 1991]. Analytic solutions employing the diffusive approximation [*Parker,* 1963] were used by *Wibberenz et al.* [1989], and approximate analytic solutions of an equation of focused transport [*Earl,* 1976] were used for a comprehensive survey of solar energetic particle observations by *Ma Sung and Earl* [1978]. *Lockwood et al.* [1982] used a Monte Carlo method to solve the hard-sphere pitch angle scattering model of *Fisk and Axford* [1969]. Numerical solutions of a diffusive model that incorporates solar wind convection and adiabatic deceleration [*Hamilton,* 1977] were also employed by *Beeck and Wibberenz* [1986] and *Beeck et al.* [1987]. Numerical solutions of the equation of focused transport of *Earl* [1976] by an eigenfunction expansion technique were used by *Bieber et al.* [1980, 1986], and solutions using a finite difference method [*Ng and Wong,* 1979; *Schlüter,* 1985] have also been employed [e.g., *Dröge et al.,* 1990b; *Kallenrode et al.,* 1992].

Naturally, a deconvolution that employs a less accurate transport model should yield a less accurate injection function. In particular, our results indicate that deconvolution with a less accurate transport model yields an artificially broad or "defocused" injection function. This underlines the importance of accurate modeling of interplanetary transport effects. A recent comparison [*Earl et al.,* 1995] showed that nearly identical results were obtained by three independent computer codes for treating interplanetary scattering, which used a Monte Carlo method [*Earl,* 1987], a finite difference method [*Ruffolo,* 1991], and an eigenfunction expansion [*Pauls and Burger,* 1994]; the consistency gives one confidence in the numerical accuracy of such methods. The transport equation and finite difference code of *Ruffolo* [1995] also include convection and adiabatic deceleration in the framework of focused transport. Solutions of this transport equation by other finite difference codes [*Hatzky,* 1996; *Lario,* 1997] and by a Monte Carlo code (L. Kocharov, private communication, 1997) have corroborated these results. Again, the agreement makes one confident that the various methods are accurately solving the transport equation. Remaining systematic errors could arise from the underlying transport assumptions.

The goal of the present work is to apply such state-of-the-art transport simulations and develop semi-automated fitting techniques to accurately determine the injection of particles near the Sun as a function of energy and time. The fits are objective, relying on χ^2 minimization instead of eyeball evaluation as in much previous work. Two deconvolution techniques have been tested for protons from the gradual flare event of July 20, 1981, and the impulsive flare event of January 2, 1982. We have successfully fit the data, and the two techniques yield consistent results. For the gradual event of July 20, 1981, the duration of injection was much shorter for protons of higher energy ($\sim$100 MeV), which we interpret as indication that the CME shock no longer accelerated protons to such high energies after traveling beyond a certain distance from the Sun.

2. Numerical Techniques

To simulate the interplanetary transport of solar energetic particles, we solve a Fokker-Planck equation of focused transport that includes the effects of interplanetary scattering, adiabatic focusing, and solar wind effects, such as solar wind convection and adiabatic deceleration, to first order in (v_{sw}/c), where v_{sw} is the (constant) solar wind speed [*Ruffolo,* 1995]:

$$\begin{aligned}
\text{streaming} \quad & \frac{\partial F}{\partial t} = -\frac{\partial}{\partial z}\mu v F \\
\text{convection} \quad & -\frac{\partial}{\partial z}\left(1-\mu^2\frac{v^2}{c^2}\right) v_{sw}\sec\psi F \\
\text{focusing} \quad & -\frac{\partial}{\partial \mu}\frac{v}{2L}\left[\frac{E'}{E}+\mu\frac{v_{sw}}{v}\sec\psi\right] \\
& \cdot(1-\mu^2)F \\
\text{differential} \quad & +\frac{\partial}{\partial \mu}v_{sw}\left(\cos\psi\frac{d}{dr}\sec\psi\right) \\
\text{convection} \quad & \cdot\mu(1-\mu^2)F \\
\text{scattering} \quad & +\frac{\partial}{\partial \mu}\frac{\varphi}{2}\frac{\partial}{\partial \mu}\frac{E'}{E}F \\
\text{deceleration} \quad & +\frac{\partial}{\partial p}p v_{sw}\left[\frac{\sec\psi}{2L}(1-\mu^2)\right. \\
& \left.+\cos\psi\frac{d}{dr}(\sec\psi)\mu^2\right]F, \qquad (1)
\end{aligned}$$

where $F(t,\mu,z,p) \equiv d^3N/(dz d\mu dp)$, the density of particles in a given magnetic flux tube (following *Ng*

and Wong [1979]) as a function of the four independent variables: t (time), μ (pitch angle cosine in the solar wind frame), z (distance along the magnetic field), and p (momentum in the solar wind frame). Also, v is the particle speed, $\psi(z)$ is the "garden hose angle" between the magnetic field and the radial direction, $L(z)$ is the focusing length, $B/(dB/dz)$, $\varphi(\mu)$ is the pitch angle diffusion coefficient, and $E'/E = 1 - \mu v_{sw} v \sec\psi/c^2$ is the ratio of the total energy in the solar wind frame to that in the fixed frame.

We assume an Archimedean spiral magnetic field [*Parker*, 1958] for the observed solar wind velocity. The pitch angle scattering coefficient, φ, is parameterized as

$$\varphi(\mu) = A|\mu|^{q-1}(1-\mu^2),$$

following *Jokipii* [1971]. We have used $q = 1.5$, which is in the range of 1.3-1.7 inferred by *Bieber et al.* [1986]. The amplitude, A was determined from $\lambda_\parallel$, the mean-free path parallel to the field, or λ_r, the radial mean free path, which are related by

$$\frac{\lambda_r}{\cos^2\psi} = \lambda_\parallel = \frac{3}{(2-q)(4-q)}\frac{v}{A}.$$

The initial condition places all the particle density at the inner boundary at $r = 0.01$ AU, simulating an instantaneous injection near the Sun. Thus the simulation results form a Green's function for the response to a δ-function injection. The initial spectrum was estimated from the data. We use absorbing (zero inflow) boundary conditions at the inner boundary and at an outer boundary far enough to be inaccessible to particles during the course of the simulation.

We numerically solved (1) using the computer code of *Ruffolo* [1995], as modified to use t instead of vt as an independent variable because data gaps can make it awkward to bin the data according to vt on a particle-by-particle basis. Simulations using t or vt as an independent variable yielded consistent results. Each simulation over the time of interest for this work required ∼4 hours on a Sun Ultra-1 workstation.

Since F is defined with respect to μ and p in the local solar wind frame, it is necessary to transform F into the fixed frame to predict counting rates. This is known as the Compton-Getting transformation [*Compton and Getting,* 1935]. We have fit data from the MEH instrument [*Meyer and Evenson,* 1978; *Kroeger,* 1986] on board the ISEE 3 spacecraft, which are collected in eight orientational sectors as the instrument's field of view (half-opening angle of 25°) rotates in the ecliptic plane. (Because of the narrow field of view of the MEH instrument, the measurements are essentially restricted to the ecliptic plane.) Therefore we used a Monte Carlo simulation to perform the Compton-Getting transformation and calculate a matrix for converting $F(\mu, p)$ into predicted counting rates in the eight sectors at the energy of interest, taking into account the geometry of the detector. The simulation also took into account the predominant magnetic field direction during the time of interest, rotating the angular distribution so that $\mu = 1$ pointed along that direction.

The simulated and observed count rates have been compared in terms of the intensity and the anisotropy times intensity. The intensity is simply the sum of the eight sectored rates. We use the anisotropy times intensity instead of the anisotropy alone because the product can be approximated by a linear combination of sectored rates, which is necessary for one of our deconvolution techniques. In general, the observed magnetic field direction and the axis of symmetry of the particle distribution both fluctuate with time, and the two do not track each other [*Bieber and Evenson,* 1987]. Presumably the axis of symmetry of the particle distribution is instead tracking a spatial average of the magnetic field over the particle gyrations. This makes it difficult to precisely predict the direction of the anisotropy, and therefore we compare the predicted and observed anisotropy times intensity values that are calculated with respect to the sector with the highest counting rate. Setting $\theta = 0$ along that sector, a first-order harmonic expansion gives $F = \langle F\rangle(1 + \delta\cos\theta)$, where θ is the angle and δ is the two-dimensional anisotropy in the ecliptic plane. Then it can readily be shown that $\delta = 2\langle\cos\theta\rangle$, where the average is weighted by the particle distribution, and the anisotropy times intensity is approximated by $2\sum_j F_j \cos\theta_j$, where F_j is the counting rate in sector j. (If the measurements were evenly distributed in three dimensions instead of two, it would be approximated by $3\sum_j F_j \cos\theta_j$.) Note that the anisotropy times intensity is calculated in the same manner for both the simulation results and the observations, so an error in the approximation should not strongly affect the comparison.

We have developed two techniques for deconvolving the effects of interplanetary transport in order to determine the underlying time profile of injection near the Sun, which in turn yields the injected spectrum as well as the best fit value of the interplanetary scattering mean-free path. These techniques solve the

inversion problem

$$R(t) = \int_0^t G(t-t')I(t')dt', \qquad (2)$$

where $I(t')$ is the injection of particles versus time near the Sun, $G(t-t')$ is the Green's function, or the response to a δ-function injection, which is calculated by the transport simulation, and $R(t)$ is the "response," i.e., the measured intensity or anisotropy times intensity at the spacecraft. Both techniques are semi-automated in that a computer program finds injection parameter values that minimize the χ^2 of the fit between $R(t)$ and the observational data (minus background). Results for different values of λ are then compared, and the overall best fit is used as the final result.

The first deconvolution technique finds the optimal piecewise linear injection function for a given set of "joints," t_i. To illustrate the technique, we consider fitting the intensity of 27-147 MeV protons measured by ISEE 3/MEH after the gradual flare event of July 20, 1981 (Figure 1a). The times of the joints in the piecewise linear injection function, $I(t')$, are chosen *a priori*, and the injection function is constrained to be zero at the first and final joints (Figure 2c). Then $I(t')$ is a linear combination of triangular injections, $I_i(t')$ (Figure 2a). The first triangular function starts from 0 at the first joint, rises linearly to 1 at the next joint, and falls linearly to 0 at the following joint (in units of 10^{26} sr^{-1} s^{-1} MeV^{-1}, i.e., 10^{26} per unit solid angle of the solar surface, time, and energy). The peak time of this function is then the start time of the next function and so on. We then convolve $G(t-t')$, the intensity predicted by the transport simulation for an instantaneous injection, with each $I_i(t')$, which yields the predicted response, $R_i(t)$, due to each triangular injection (Figure 2b). Now we want to consider the response, $R(t)$, to a general linear combination of the triangular injections. Because the transport equation is linear in F, the response to a linear combination of injections, $I(t') = \sum_i a_i I_i(t')$, is the linear combination of responses, $R(t) = \sum_i a_i R_i(t)$. Therefore we can use linear least-squares fitting to find the linear combination that minimizes the χ^2 between $R(t)$ and the observed data (Figure 2d). Because each $I_i(t')$ has a peak value of one, the coefficients, a_i, are the values of the injection function at each joint t_i (Figure 2c); the least squares fit also directly yields the statistical errors of these values.

Initially, we set t_0 to the peak time of the Hα flare, set t_1 and t_2 so that $t_2 - t_1$ and $t_1 - t_0$ were equal to the width of the time bins of the data, and set further t_i so that each interval was twice the preceding interval. The joints, t_i, were then adjusted according to an objective procedure. While the procedure could have been fully automated, we considered it prudent to manually execute fits for each set of joints, examining each fit by eye; we never found it necessary to contradict the decisions mandated by this procedure. Each fit runs in the blink of an eye on a Pentium processor and the fitting procedure is completed in minutes.

The second deconvolution technique assumes an injection function of the form

$$I(t) = [C/(t-t_0)] \exp[-A/(t-t_0) - (t-t_0)/B],$$

where A, B, C, and t_0 are free parameters. This form was originally proposed by *Reid* [1964] as the solution of a coronal diffusion equation over the solar surface. However, we adopt this so-called Reid profile only as a convenient and widely understood parameterization, and we stress that we do not assume the existence of coronal diffusion.

We perform a nonlinear least squares fit in which for each set of parameter values, A, B, and t_0, we numerically evaluate $R(t)$ from (2) using the results of the transport simulation, and calculate χ^2 for the fit to the data. (Given the other parameters, the optimal value of C can readily be determined.) The parameters are optimized by the conjugate direction method [*Press et al.,* 1988]. In practice, it was necessary to limit the variation of A, B, and t_0 to physically reasonable values. Unfortunately, for nonlinear optimization, one cannot be certain that the global minimum has been found, and we had to restart each fit several times for different initial parameter values. Fits were performed for various values of λ so as to optimize χ^2. Each fit required ~ 2 hours on a Pentium processor, making the entire procedure much slower than the piecewise linear technique. Although both deconvolution techniques yielded good fits and consistent results, we prefer the piecewise linear deconvolution technique, which is faster, does not require any subjective evaluation by the researcher, and permits a more flexible shape for the injection function.

3. Observations and Results

We have examined data on protons stopping in the ISEE 3/MEH detector. During the times considered here, ISEE 3 was located near the inner Sun-Earth Lagrangian point. Two types of data have been used.

Priority rate (PR) data consist of raw counts in eight directional sectors over 96 s intervals that satisfy the priority 1 logic ($D1 \times D3 \times \overline{D2 + D13A} \times \overline{\gamma H} \times \overline{D5} \times \overline{D6}$ [*Kroeger,* 1986]). It expected that during an intense solar event this rate is dominated by protons (other ions and electrons have priority 2), and detector simulations indicate that the stopping energies are roughly 27-147 MeV. Large PR counting rates may have a very small statistical error, yet there are still fluctuations that are probably related to magnetic field irregularities. In that case, the statistical errors do not reflect the true level of effectively random rate fluctuations, leading to large χ^2 values even for a reasonable fit. Pulse height (PH) data enable one to reject background events more cleanly and also to determine the energy (within $\sim$ 1 MeV) and time of arrival of each particle. While such data are clearly more desirable, the transmission of PH data to Earth was constrained by telemetry limits and depended on the priority logic. One must correct for this, and during times with a large electron flux, the PH data may yield poor statistics for the lower-priority protons.

We chose to test the deconvolution techniques using data for two solar events, one impulsive (X ray duration $<$ 1 hour) and one gradual (X ray duration $>$ 1 hour). Thus the objective is to examine events for which the particles are evidently of solar origin, and are sufficiently intense to permit a detailed analysis and for which there is an evident anisotropy, which is an aspect of the fitting we would like to test. Other considerations are the absence of data gaps at the very start of the event and a small coronal distance between flare site and the footpoint of the (average) magnetic field connected to the spacecraft. We chose to examine the gradual event of July 20, 1981, and the impulsive event of January 2, 1982. Starting with such "well-connected" events simplifies the interpretation of the results; in future applications one could use these deconvolution techniques for poorly connected events in order to study lateral transport mechanisms.

Figure 1 shows PR proton data for the gradual event of July 20, 1981. This event was associated with an Hα flare at 25°S, 75°W, peaking at 1322-1336 UT (based on two observatories, Solar-Geophysical Data). The X ray decay time was 67 min [*Cliver et al.,* 1989], indicating a gradual flare. The solar wind speed was approximately 375 km s^{-1} (S. Bame, private communication via ISEE 3 data pool, 1981). The magnetic field varied rapidly in both magnitude and direction during the time of interest (E. Smith, private communication via ISEE 3 data pool, 1981).

Although the intensity was rather smooth as a function of time, the anisotropy times intensity suddenly fell by a factor of about 4 at 1600 UT and recovered at 1700 UT. Such sudden disappearances of anisotropy have been observed for other flare events by *Evenson et al.* [1982]. As discussed earlier, the anisotropy vector closely follows the magnetic field direction, so it would be expected to be especially sensitive to erratic magnetic field fluctuations. In fact, the field magnitude dropped particularly sharply during 1600-1700 UT, corresponding to a very short focusing length, $L \equiv -B/(dB/dz) \approx -0.04$ AU; this strong reverse focusing apparently negated most of the outward-going anisotropy during that time. It is impossible for a transport model based on an Archimedean spiral field to predict such drastic fluctuations in the anisotropy. Therefore we conclude that when the magnetic field is erratic, as for this flare, our transport simulations are only appropriate for fitting the intensity as a function of time and particle energy.

For the proton event of July 20, 1981, there were sufficient statistics to use PH data and to separately examine different proton energy ranges. Fits were performed using both a piecewise linear injection profile and a Reid profile, assuming a position-independent radial mean free path, λ_r, as recommended by *Palmer* [1982]. The resulting fit parameters are given in Tables 1 and 2, and piecewise linear injection functions are shown in Figure 3. In each case, both deconvolution techniques yielded the same best fit value of λ_r, except for the highest energy bin where they differed slightly. There is a hint of an increasing trend of λ_r with energy, which is consistent with previous results and theoretical calculations [e.g., *Dröge et al.,* 1997; *Schmidt and Dröge,* 1997] The injection functions can be compared in terms of the full width at half maximum (FWHM). While the Reid profile always has a higher FWHM, the energy dependence is similar for both methods.

Tables 1

Figure 3

Both deconvolution techniques indicate a much narrower injection profile for the highest energy bin (75-147 MeV). As discussed earlier, there is evidence that for gradual events the acceleration of ions takes place at a CME-driven shock as it propagates outward through the corona. Therefore the injection as a function of time can also be interpreted as injection as a function of distance [*Kahler et al.,* 1990], though the CME speed is not known for this particular event. Thus these results suggest that for this

event the CME/shock system lost the ability to accelerate particles to ∼100 MeV after traveling beyond a certain distance from the Sun.

By integrating the injection function over time for each energy bin, we can estimate the spectrum of emitted particles. We compare our techniques with the commonly used time of maximum (TOM) method, in which one uses the observed peak intensity for each energy interval to estimate the relative spectrum. For the July 20, 1981, event, we find that the piecewise linear and Reid injection profiles yield very similar absolute spectra, except at the highest energies (Table 3). The relative spectra of both methods are also similar to the TOM spectrum, except at the high energy bin. The TOM technique implicitly assumes a similar injection profile and scattering mean-free path for each energy, so one might well expect some deviation for the high energy bin, where both deconvolution techniques yield a much shorter duration of injection. Also, there were large statistical errors for this energy bin. From our results we conclude that the TOM relative spectrum can be accurate for a short energy span (here a factor of 3), but for wider energy ranges it is worthwhile to determine the spectrum more accurately by deriving the energy-dependent injection profiles. Note that the TOM method does not yield an absolute spectrum, and the consistency of our two methods for the absolute spectrum improves our confidence in both of them.

We have also analyzed PR data from the impulsive flare event of January 2, 1982 (Figure 4). This event was associated with an Hα flare at 18°S, 88°W, peaking at 0620-0621 UT (Solar-Geophysical Data). The X ray decay time was 16 min [*Cliver et al.,* 1989], and the solar wind speed was approximately 350 km s^{-1} (S. Bame, private communication via ISEE 3 data pool, 1982). The magnetic field was stable in magnitude and direction during the time of interest (E. Smith, private communication via ISEE 3 data pool, 1982). Because of this, we were able to analyze the anisotropy in addition to the intensity for this event. Unfortunately, because of the limited statistics and strong intensity of electrons (which had a higher priority for pulse-height telemetry), we were unable to examine PH data in detail to determine energy-dependent injection functions.

Simultaneously fitting the intensity and anisotropy times intensity provides a stringent test of the injection and transport models. Our two techniques for deconvolving the effects of interplanetary transport yielded similar FWHM durations of injection (17 and 24 min, respectively; see Tables 1 and 2) and yielded reasonable fits to the intensity and anisotropy times intensity. The duration of injection over this broad energy range (27-147 MeV) was similar to the decay time of X ray emission (16 min) and was markedly shorter than the corresponding duration for the gradual event of July 20, 1981, though that event had a similarly short injection duration for the highest energies.

We close this section with examples of how less accurate transport assumptions can artificially broaden the derived injection profile. For an analogy, consider the deconvolution of a telescope image to account for the point spread function. An inaccurate estimate of the point spread function yields a deconvolved image that is still artificially broad compared to the true image size. When an improved point spread function is used, one obtains a sharper image.

Figure 5 shows examples of a similar effect for our deconvolution problem, in which we compare fits to PR data from both events, assuming that either λ_r or $\lambda_\parallel$ is constant in position. Previous authors [e.g., *Palmer,* 1982] have concluded that a constant λ_r is a better and reasonable assumption for transport in the inner heliosphere. We find that the fits assuming a constant $\lambda_\parallel$ (Figures 5c and 5d) yield much broader injection functions than those based on the presumably more accurate assumption of a constant λ_r (Figures 5a and 5b). These examples stress the importance of using an accurate transport model when determining the injection function near the Sun.

4. Discussion

The previous study with goals most similar to ours was that of *Ma Sung and Earl* [1978], which employed approximate analytic solutions to a focused transport equation. One of their assumptions was a position-independent ratio, $\lambda_\parallel/L$, where L is the focusing length. This assumption was necessary for their analytic approximation but is less accurate than the assumption of a constant λ_r and a function $L(z)$ derived for an Archimedean field. Based on our results, one would expect injection functions that are smeared out when compared with those for a constant λ_r (Figure 5). Those authors frequently found particle release times of the order of hours, and it is possible that their injection profiles were artificially broad due to that assumption. The deconvolution techniques presented here, along with more realistic

transport assumptions and modern numerical simulations, could be profitably applied to survey the injection profiles of a variety of events, as *Ma Sung and Earl* [1978] did. Shortly, we will consider how such results should be interpreted in light of our modern understanding of the origin of solar energetic particles.

A valid question is how one knows that injection occurs near the Sun, when the interplanetary shocks that frequently accompany gradual events are known to be capable of accelerating particles [*Gosling et al.,* 1981]. For the gradual event considered here, several days after the flare, the log(proton intensity) versus time showed a bump (July 23) and then a double-peaked increase (July 24-25) to fluxes <1/30 of the initial peak. There was intense geomagnetic activity at these times (Solar-Geophysical Data). Presumably these features are associated with the passage of a CME/shock system, which affected the particle propagation or accelerated particles to higher energies. In this work, we focus on the proton observations on July 20-21, 1981, well before such features arose. The rapid rise and exponential decline are consistent with injection shortly after the flare occurrence convolved with the effects of interplanetary transport. Since the CME could not have traveled far from the Sun during that time, we concluded that the emission was near the Sun and neglected any source motion.

We note further that all measurements of ionic charge states above 3 MeV/nucleon indicate that solar energetic ions are accelerated out of coronal material [*Boberg et al.,* 1996]. This implies that the CME/shock system first accelerates ions out of coronal material, presumably while it is still near the Sun, and can also further accelerate ions as it propagates outward. The relative importance of acceleration at different distances from the Sun undoubtedly varies from event to event and varies with energy.

Our results indicate that for the gradual event of July 20, 1981, the duration of injection was much shorter for higher energies (Figure 3), which implies that the CME/shock system lost the ability to accelerate a significant flux of ∼100 MeV protons after traveling a certain distance from the Sun. We also note that the shock-associated particle increases on July 23, and July 24-25 had a significantly steeper spectrum than the main peak on July 20 and were not seen at all in the high energy bin. Therefore one might interpret the short duration of injection at higher energy as indicating a transition from injection with a harder spectrum (when the CME shock is close to the Sun) to injection with a softer spectrum (as for the interplanetary shock). While it is imprudent to draw general conclusions from one flare/CME event, confirmation of this result for other events would provide important information on the acceleration mechanism for escaping energetic ions from such events.

It is also interesting to compare the best fit values of λ for fits assuming a constant $\lambda_\parallel$ or a constant λ_r, which are largely determined by the observed intensity decay at long times. We obtain ratios of $\lambda_\parallel/\lambda_r = 5.8$ and 4.5 (Table 1). At any given point, $\lambda_\parallel/\lambda_r = \sec^2\psi$, so the observed ratios are characteristic of $r = 1.9$ and 1.5 AU. This indicates that the intensity versus time of solar particles at 1 AU is strongly influenced by the transport conditions at greater distances.

Since we have only treated the interplanetary transport parallel to the magnetic field, we have derived injection profiles under the assumption that particles are strictly confined to a narrow flux tube connecting the observer to the source near the Sun. However, perpendicular diffusion implies that the observed particles could have originated from a distribution of longitudes and latitudes. Summarizing a variety of results, *Palmer* [1982] recommends using $\kappa_\perp = (v/c) \times 10^{21}$ cm^2 s^{-1} at 1 AU (well away from sector boundaries, corotating interaction regions, etc.). For our typical proton velocity of $c/3$, this implies an angular spread of ∼7° after 3 hour or ∼20° after 1 day. In comparison, gradient and curvature drifts imply an angular motion ∼0.1 AU day^{-1} near the Earth or an integrated angular motion ∼0.1° for the first particles that arrive and are hence negligible during the time of interest, as is the rotation of the Sun.

For gradual events, there is evidence that coronal mass ejection shocks can accelerate and release particles over a large fraction of the solar surface [*Mason et al.,* 1984; *Kahler,* 1992], so our results are really telling us the injection profile averaged over ∼ 7° of solar latitude and longitude from the footpoint magnetically connected to the observer (which is itself uncertain, except when there are observations of moving interplanetary type III radio bursts that track the mean motion of electrons along the interplanetary magnetic field [*Reames and Stone,* 1986; *Reiner et al.,* 1995]). The accuracy of the measured duration of injection as a function of energy should be unaffected insofar as perpendicular diffusion does not significantly increase the distance traveled before particles actually reach the observer, i.e., as long as it is much weaker than parallel diffusion.

For impulsive events, the interpretation is potentially more complex: Since particles are accelerated at the flare site, their lateral spread could be due to perpendicular diffusion in the interplanetary magnetic field (including the "random walk" of the magnetic field lines themselves [e.g., *Jokipii,* 1966; *Matthaeus et al.,* 1995]) or to lateral transport within the corona. For impulsive flares that are magnetically well-connected to the observer, such as the event of January 2, 1982, which we have considered here, we can again argue that our determination of the duration of injection is accurate as long as perpendicular diffusion does not significantly increase the propagation time. However, the absolute normalization of the observed flux depends strongly on the lateral extent of the particle distribution at the observer's radius. In this case, we are determining the number of particles injected per solid angle at the observer's radius.

5. Conclusions

We have developed two techniques for deconvolving the effects of interplanetary transport using numerical solutions of the transport equation: (1) assuming a piecewise linear injection profile and (2) using a Reid injection profile. The deconvolution can yield the interplanetary scattering mean free path, the injection profile as a function of energy, and the spectrum. The two techniques yield consistent results for the gradual flare/CME event of July 20, 1981, and the impulsive flare event of January 2, 1982, giving us confidence in both techniques. The piecewise linear profile is preferred because the fitting procedure is faster, objective (not relying on user evaluation of fits), and permits a more flexible profile shape. It is important to examine the observed magnetic field; if this is erratic, it may not be possible to fit the anisotropy data with simple transport assumptions. For the July 20, 1981, event, a simple time-of-maximum estimate of the spectrum agreed with our results over a factor of 3 in energy but deviated at higher energies. The FWHM of injection was much shorter for higher energies ($\sim$100 MeV), indicating that for this event, the CME and associated shock lost their efficiency of accelerating such particles after traveling a certain distance from the Sun.

Acknowledgments. The authors would like to thank Paul Evenson and Peter Meyer for stimulating discussions and for providing the ISEE 3 data. We are also grateful for useful discussions with Wolfgang Dröge and John Bieber. This work was partially supported by grants from Chulalongkorn University's Rachadapisek Sompoj Fund and the Thailand Research Fund. TK also received support from a Naresuan University Scholarship.

The Editor thanks M. Aschwanden and another referee for their assistance in evaluating this papaer.

References

Aschwanden, M. J., Electron versus proton timing delays in solar flares, *Astrophys. J., 470,* L69-L72, 1996.

Aschwanden, M. J., A. O. Benz, B. R. Dennis, and M. R. Kundu, Pulsed acceleration in solar flares, *Astrophys. J. Suppl. Ser., 90,* 631-638, 1994.

Beeck, J., and G. Wibberenz, Pitch angle distributions of solar energetic particles and the local scattering properties of the interplanetary medium, *Astrophys. J., 311,* 437-450, 1986.

Beeck, J., G. M. Mason, D. C. Hamilton, G. Wibberenz, H. Kunow, D. Hovestadt, and B. Klecker, A multi-spacecraft study of the injection and transport of solar energetic particles, *Astrophys. J., 322,* 1052-1072, 1987.

Bieber, J. W., and P. Evenson, Correlation of variations in the angular distribution of 50 MeV particles with magnetic field fluctuations, *Proc. Int. Cosmic Ray Conf., 20th, 3,* 151-154, 1987.

Bieber, J. W., J. A. Earl, G. Green, H. Kunow, R. Müller-Mellin, and G. Wibberenz, Interplanetary pitch angle scattering and coronal transport of solar energetic particles: New information from Helios, *J. Geophys. Res., 85*, 2313-2323, 1980.

Bieber, J. W., P. A. Evenson, and M. A. Pomerantz, Focusing anisotropy of solar cosmic rays, *J. Geophys. Res., 91,* 8713-8724, 1986.

Boberg, P. R., A. J. Tylka, and J. H. Adams, Jr., Solar energetic Fe charge state measurements: Implications for acceleration by coronal mass ejection-driven shocks, *Astrophys. J., 471,* L65-L68, 1996.

Chupp, E. L., Transient particle acceleration associated with solar flares, *Science, 250,* 229-236, 1990.

Cliver, E. W., D. J. Forrest, H. V. Cane, D. V. Reames, R. E. McGuire, T. T. von Rosenvinge, S. R. Kane, and R. J. MacDowall, Solar flare nuclear gamma-rays and interplanetary proton events, *Astrophys. J., 343,* 953-970, 1989.

Compton, A. H., and I. A. Getting, An apparent effect of galactic rotation on the intensity of cosmic rays, *Phys. Rev., 2nd Ser., 47,* 817-821, 1935.

Debrunner, H., E. Flückiger, H. Grädel, J. A. Lockwood, and R. E. McGuire, Observations related to the acceleration, injection, and interplanetary propagation of energetic protons during the solar cosmic ray event on February 16, 1984, *J. Geophys. Res., 93,* 7206-7216, 1988.

Debrunner, H., et al., Energetic neutrons, protons, and gamma rays during the 1990 May 24 solar cosmic ray event, *Astrophys. J., 479,* 997-1011, 1997.

Dröge, W., D. J. Forrest, and B. Klecker, Solar flare electron and gamma ray spectra, *Proc. Int. Cosmic Ray Conf., 21st, 5,* 84-87, 1990a.

Dröge, W., G. Wibberenz, and B. Klecker, A dual spacecraft study of the injection and propagation of energetic particles following the 7 June 1980 gamma ray flares, *Proc. Int. Cosmic Ray Conf., 21st, 5,* 187-190, 1990b.

Dröge, W., D. Ruffolo, and T. Khumlumlert, The rigidity dependence of solar electron mean free paths in the range 0.3 to 20 MV, *Proc. Int. Cosmic Ray Conf., 25th, 1,* 137-140, 1997.

Earl, J. A., The effect of adiabatic focusing upon charged-particle propagation in random magnetic fields, *Astrophys. J., 205,* 900-919, 1976.

Earl, J. A., Charged particle transport calculations on the massively parallel processor, *Proc. Int. Cosmic Ray Conf., 20th, 3,* 198-201, 1987.

Earl, J. A., D. Ruffolo, H. L. Pauls, and J. W. Bieber, Comparison of three numerical treatments of charged particle transport, *Astrophys. J., 454,* 749-761, 1995.

Evenson, P., P. Meyer, and S. Yanagita, Solar flare shocks in interplanetary space and solar flare particle events, *J. Geophys. Res., 87,* 625-631, 1982.

Fisk, L. A., ^{3}He-rich flares: A possible explanation, *Astrophys. J., 224,* 1048-1055, 1978.

Fisk, L. A., and W. I. Axford, Anisotropies of solar cosmic rays, *Sol. Phys., 7,* 486-498, 1969.

Gosling, J. T., J. R. Asbridge, S. J. Bame, W. C. Feldman, R. D. Zwickl, G. Paschmann, N. Sckopke, and R. J. Hynds, Interplanetary ions during an energetic storm particle event: The distribution function from solar wind thermal energies to 1.6 MeV, *J. Geophys. Res., 86,* 547-554, 1981

Hamilton, D. C., The radial transport of energetic solar flare particles from 1 to 6 AU, *J. Geophys. Res., 82,* 2157-2169, 1977.

Hatzky, R., Winkelverteilungen energiereicher geladener Teilchen und die Streueigenschaften des interplanetaren Mediums, Ph.D. thesis, 247 pp., Univ. Kiel, Kiel, Germany, Oct. 1996.

Hsieh, K. C., and J. A. Simpson, The relative abundances and energy spectra of ^{3}He and ^{4}He from solar flares, *Astrophys. J., 162,* L191-L196, 1970.

Jokipii, J. R., Cosmic-ray propagation, I, Charged particles in a random magnetic field, *Astrophys. J., 146,* 480-487, 1966.

Jokipii, J. R., Propagation of cosmic rays in the solar wind, *Rev. Geophys., 9*, 27-87, 1971.

Kahler, S. W., Solar flares and coronal mass ejections, *Ann. Rev. Astron. Astrophys., 30,* 113-141, 1992.

Kahler, S. W., D. V. Reames, and N. R. Sheeley Jr., Coronal mass ejections and the injection profiles of solar energetic particle events, *Proc. Int. Cosmic Ray Conf., 21st, 5,* 183-186, 1990.

Kallenrode, M.-B., and G. Wibberenz, Particle injection following solar flares on 1980 May 28 and June 8: Evidence for different injection time histories in impulsive and gradual events?, *Astrophys. J., 376,* 787-796, 1991.

Kallenrode, M.-B., G. Wibberenz, and S. Hucke, Propagation conditions of relativistic electrons in the inner heliosphere, *Astrophys. J., 394,* 351-356, 1992.

Kroeger, R., Measurements of hydrogen and helium isotopes in galactic cosmic rays from 1978 through 1984,

Astrophys. J., 303, 816-828, 1986.

Lario, D., Propagation of low-energy particles through the interplanetary medium: Modeling their injection from interplanetary shocks, Ph.D. thesis, 294 pp., Univ. Barcelona, Barcelona, Spain, July 1997.

Lee, M. A., and J. M. Ryan, Time-dependent coronal shock acceleration of energetic solar flare particles, *Astrophys. J., 303,* 829-842, 1986.

Leske, R. A., J. R. Cummings, R. A. Mewaldt, E. C. Stone, and T. T. von Rosenvinge, Measurements of the ionic charge states of solar energetic particles using the geomagnetic field, *Astrophys. J., 452,* L149-L152, 1995.

Lockwood, J. A., H. Debrunner, E. Flückiger, H. Neuenschwander, and M. Schubnell, A model of propagation of solar flare particles and its application to cosmic ray ground level events, *J. Geophys. Res., 87,* 4338-4344, 1982.

Luhn, A., B. Klecker, D. Hovestadt, G. Gloeckler, F. M. Ipavich, M. Scholer, C. Y. Fan, and L. A. Fisk, Ionic charge states of N, Ne, Mg, Si and S in solar energetic particle events, *Adv. Space Res., 4,* No. 2-3, 161-164, 1984.

Luhn, A., B. Klecker, D. Hovestadt, and E. Möbius, The mean ionic charge of silicon in ^{3}He-rich solar flares, *Astrophys. J., 317,* 951-955, 1987.

Mason, G. M., G. Gloeckler, and D. Hovestadt, Temporal variations of nucleonic abundances in solar flare energetic particle events, II, Evidence for large-scale shock acceleration, *Astrophys. J., 280,* 902-916, 1984.

Mason, G. M., J. E. Mazur, M. D. Looper, and R. A. Mewaldt, Charge state measurements of solar energetic particles observed with SAMPEX, *Astrophys. J., 452,* 901-911, 1995.

Ma Sung, L. S., and J. A. Earl, Interplanetary propagation of flare-associated energetic particles, *Astrophys. J., 222,* 1080-1096, 1978.

Matthaeus, W. H., P. C. Gray, D. H. Pontius, Jr., and J. W. Bieber, Spatial structure and field-line diffusion in transverse magnetic turbulence, *Phys. Rev. Lett., 75,* 2136-2139, 1995.

Meyer, P., and P. Evenson, The University of Chicago cosmic ray electrons and nuclei experiment on the H spacecraft, *IEEE Trans. Geosci. Electron., 16*, 180-185, 1978.

Meyer, P., E. N. Parker, and J. A. Simpson, Solar cosmic rays of February, 1956 and their propagation through interplanetary space, *Phys. Rev., 104,* 768-783, 1956.

Ng, C. K., and K.-Y. Wong, Solar particle propagation under the influence of pitch-angle diffusion and collimation in the interplanetary magnetic field, *Proc. Intl. Cosmic Ray Conf., 16th, 5,* 252-257, 1979.

Oetliker, M., B. Klecker, D. Hovestadt, G. M. Mason, J. E. Mazur, R. A. Leske, R. A. Mewaldt, J. B. Blake, and M. D. Looper, The ionic charge of solar energetic particles with energies of 0.3-70 MeV per nucleon, *Astrophys. J., 477,* 495-501, 1997.

Pallavicini, R., S. Serio, and G. S. Vaiana, A survey of soft X-ray limb flare images: The relation between their structure in the corona and other physical parameters, *Astrophys. J., 216,* 108-122, 1977.

Palmer, I., Transport coefficients of low-energy cosmic rays in interplanetary space, *Rev. Geophys. Space Phys., 20,* 335-351, 1982.

Parker, E. N., Dynamics of the interplanetary gas and magnetic fields, *Astrophys. J., 128,* 664-676, 1958.

Parker, E. N., *Interplanetary Dynamical Processes,* 272 pp., Wiley-Interscience, New York, 1963.

Pauls, H. L., and R. A. Burger, Eigenfunction solution of Boltzmann's equation for the case of a focusing magnetic field with finite helicity, *Astrophys. J., 427,* 927-931, 1994.

Press, W. H., B. P. Flannery, S. A. Teukolsky, and W. T. Vetterling, *Numerical Recipes in C,* 735 pp., Cambridge Univ. Press, New York, 1988.

Rank, G., H. Debrunner, L. Kocharov, G. Kovaltsov, J. Lockwood, M. McConnell, P. Nieminen, J. Ryan, and V. Schönfelder, The solar flare on 15 June 1991, *Proc. Int. Cosmic Ray Conf., 25th, 1,* 1-4, 1997a.

Rank, G., H. Debrunner, J. Lockwood, M. McConnell, J. Ryan, and V. Schönfelder, Extended gamma-ray emission of the solar flares in June 1991, *Proc. Int. Cosmic Ray Conf., 25th, 1,* 5-8, 1997b.

Reames, D. V., Acceleration of energetic particles by shock waves from large solar flares, *Astrophys. J., 358,* L63-L67, 1990.

Reames, D. V., and R. G. Stone, The identification of solar ^{3}He-rich events and the study of particle acceleration at the Sun, *Astrophys. J., 308,* 902-911, 1986.

Reid, G. C., A diffusive model for the initial phase of a solar proton event, *J. Geophys. Res., 69,* 2659-2667, 1964.

Reiner, M. J., J. Fainberg, and R. G. Stone, Large-scale interplanetary magnetic field configuration revealed by solar radio bursts, *Science, 270,* 461-464, 1995.

Ruffolo, D., Interplanetary transport of decay protons from solar flare neutrons, *Astrophys. J., 382,* 688-698, 1991.

Ruffolo, D., Effect of adiabatic deceleration on the focused transport of solar cosmic rays, *Astrophys. J., 442,* 861-874, 1995.

Ruffolo, D., Charge states of solar cosmic rays and constraints on acceleration times and coronal transport, *Astrophys. J., 481,* L119-L122, 1997.

Schlüter, W., Die numerische Behandlung der Ausbreitung solarer flareinduzierter Teilchen in den magnetischen Feldern des interplanetaren Raumes, Ph.D. thesis, 147 pp., Univ. Kiel, Kiel, Germany, Nov. 1985.

Schmidt, J., and W. Dröge, Scattering of cosmic rays at MHD waves with different cross helicity and polarization, *Proc. Intl. Cosmic Ray Conf., 25th, 1,* 221-224, 1997.

Sheeley, N. R., Jr., R. A. Howard, M. J. Koomen, and

D. J. Michels, Associations between coronal mass ejections and soft X-ray events, *Astrophys. J., 272,* 349-354, 1983.

Wibberenz, G., K. Kecskeméty, H. Kunow, A. Somogyi, B. Iwers, Y. I. Logachev, and V. G. Stolpovskii, Coronal and interplanetary transport of solar energetic protons and electrons, *Sol. Phys., 124,* 353-392, 1989.

D. Ruffolo and W. Youngdee, Department of Physics, Chulalongkorn University, Bangkok 10330, Thailand. (e-mail: david@astro.phys.sci.chula.ac.th)

T. Khumlumlert, Department of Physics, Naresuan University, Phitsanulok 65000, Thailand. (e-mail: thiraneek@nu.ac.th)

January 28, 1998; revised March 12, 1998; accepted April 15, 1998.

[1]Now at Department of Physics, Naresuan University, Phitsanulok, Thailand.

This preprint was prepared with AGU's LaTeX macros v4. File duration formatted February 1, 2008.

Figure 1. Intensity and anisotropy times intensity as a function of time for 27-147 MeV protons following the July 20, 1981, gradual solar flare event.

Figure 2. Illustration of the deconvolution technique for a piecewise linear injection function near the Sun. The transport equation is solved for an instantaneous injection of particles. The resulting Green's function is convolved with (a) triangular injection profiles to (b) yield response functions. Linear, least squares fitting yields (d) the linear combination of response functions that best fits the data and (c) the corresponding best-fit piecewise linear injection profile.

Figure 3. Fits to the (a) observed proton intensity versus time in four energy bins for (b) optimal piecewise linear injection profiles. Note the expanded timescale in the right panels.

Figure 4. Fits to the (a) observed 27-147 MeV proton intensity versus time and anisotropy times intensity versus time for the (b) optimal piecewise linear injection profile. Note the expanded timescale in Figure 4b.

Figure 5. Comparison of best-fit piecewise linear injection profiles for transport simulations assuming either (a-b) λ_r or (c-d) $\lambda_\parallel$ to be independent of position for 27-147 MeV protons on July 20, 1981, for Figures 5a and 5c and January 2, 1982, for Figures 5b and 5d. The assumption of a constant λ_r is expected to be more accurate, and it yields a sharper injection function for both events.

Table 1. Fit Parameters for a Piecewise Linear Injection Profile

Date	Data	Energy, MeV	λ_r or $\lambda_\parallel$ constant?	λ, AU	$\{a_i\}$[a]	χ^2/d.f.	FWHM, min	Figure
July 20, 1981	PH	27-39	λ_r	0.08	$\{7.2, 0.5, 0.7\}$	1.92	33	3
	PH	39-55	λ_r	0.10	$\{1.6, 1.9\}$	0.96	65	3
	PH	55-75	λ_r	0.12	$\{0.57, 0.93\}$	1.11	52	3
	PH	75-147	λ_r	0.10	$\{0.58, 0.04\}$	1.24	12	3
	PR	27-147	λ_r	0.12	$\{1.095, 0.089, 0.120\}$	161.65	31	2, 5
	PR	27-147	$\lambda_\parallel$	0.70	$\{0.296, 0.503, 0.414, 0.0942\}$	89.68	156	5
Jan. 2, 1982	PR	27-147	λ_r	0.20	$\{12.0, 2.7\}\times10^{-3}$	2.09	17	4, 5
	PR	27-147	$\lambda_\parallel$	0.90	$\{2.8, 4.1, 3.3, 2.1, 1.0\}\times10^{-3}$	2.35	52	5

[a]Units of 10^{26} sr^{-1} s^{-1} MeV^{-1}.

Table 2. Fit Parameters for a Reid Injection Profile

Date	Data	Energy, MeV	λ_r, AU	A, min	B, min	C[a]	t_0, UT	χ^2/d.f.	FWHM, min
July 20, 1981	PH	27-39	0.08	23.6	81.7	436.8	1330	2.43	47
	PH	39-55	0.10	96.0	44.5	1586.4	1314	1.11	68
	PH	55-75	0.12	54.6	46.7	251.0	1325	1.18	55
	PH	75-147	0.12	22.6	30.0	30.5	1324	0.99	29
Jan. 2, 1982	PR	27-147	0.20	96.7	9.0	165.4	0535	3.70	24

[a]Units of 10^{26} sr^{-1} s^{-1} MeV^{-1}.

Table 3. Spectra of Protons Injected on July 20, 1981

Technique	Energy Range, MeV			
	27-39	39-55	55-75	75-147
Absolute Spectra, 10^{26} sr^{-1} s^{-1} MeV^{-1}				
Piecewise linear	19,000	7120	2770	465
Reid profile	19,900	7120	2810	581
Relative Spectra				
Piecewise linear	1	0.374	0.145	0.0244
Reid profile	1	0.358	0.141	0.0292
Time of maximum	1	0.343	0.136	0.0185

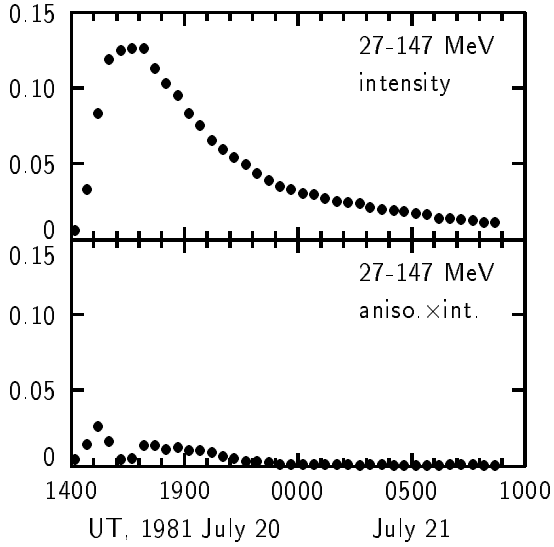
0.15
0.10
0.05
0
27-147 MeV
intensity
0.15
0.10
0.05
0
27-147 MeV
aniso.×int.
1400
1900
0000
0500
1000
UT, 1981 July 20
July 21

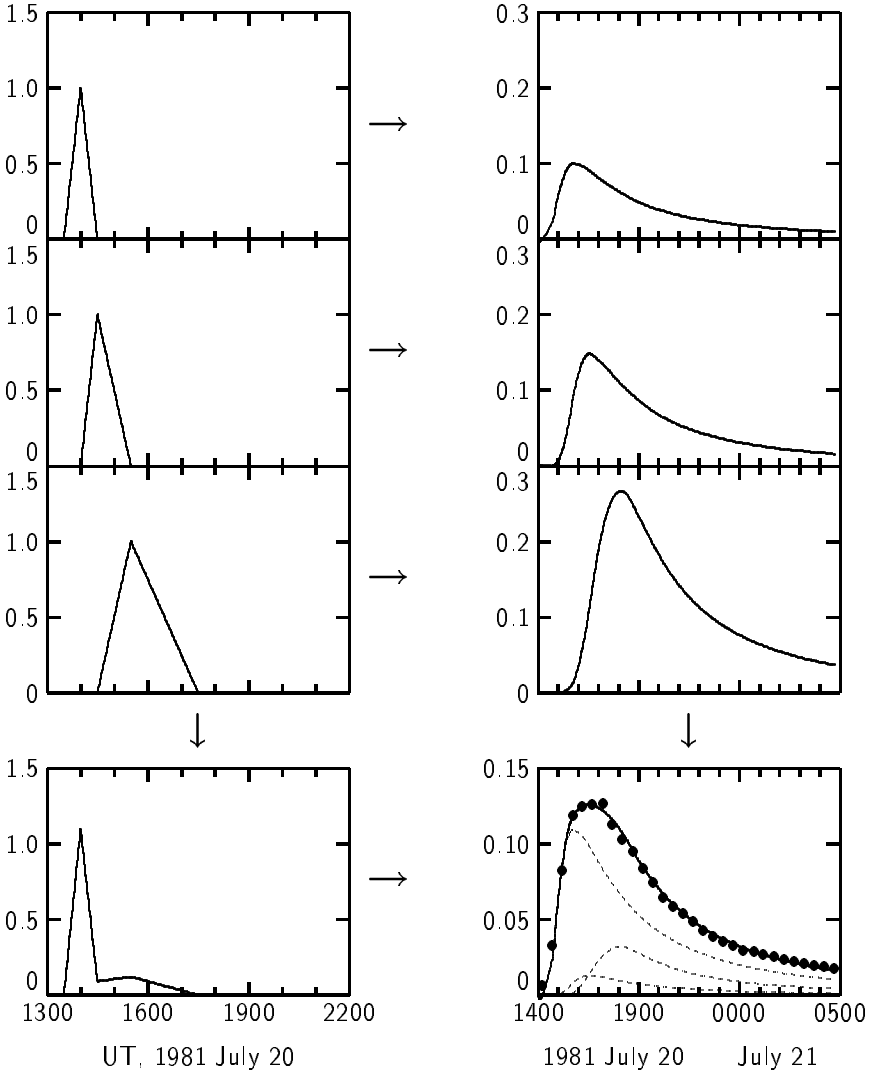
1.5
1.0
0.5
0
0.3
0.2
0.1
0.15
0.10
0.05
1300
1600
1900
2200
1400
0000
0500
UT, 1981 July 20
1981 July 20
July 21

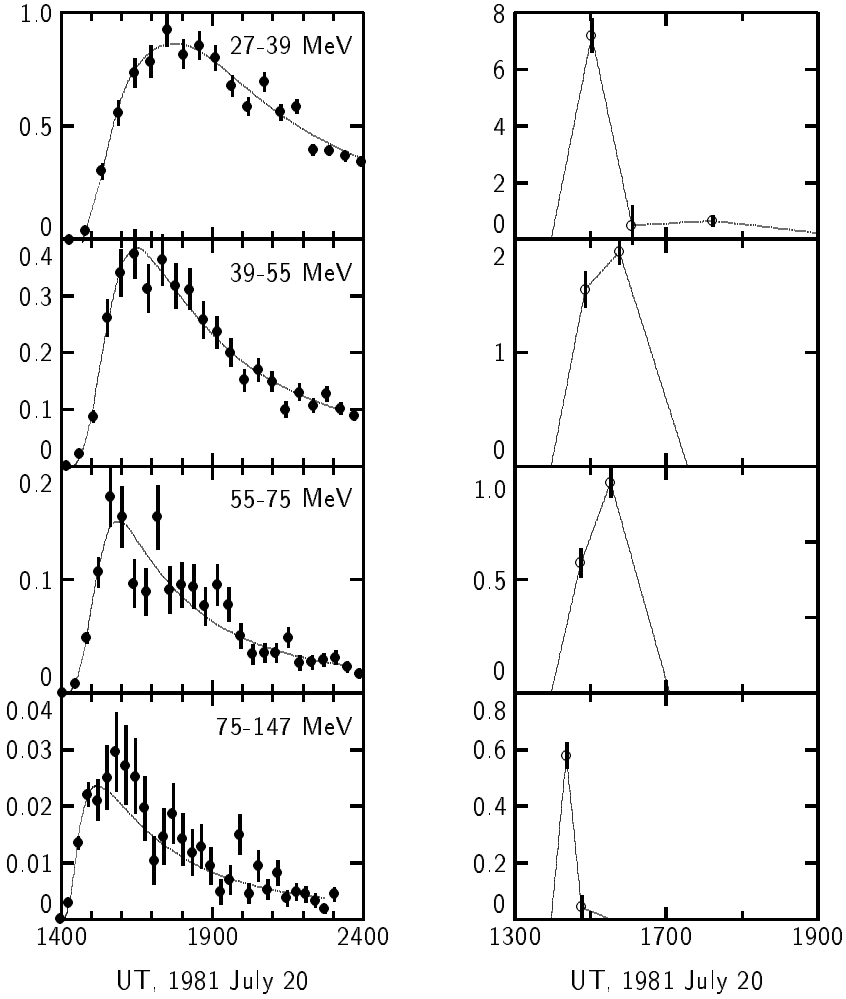
27-39 MeV
39-55 MeV
55-75 MeV
75-147 MeV
1400
1900
2400
UT, 1981 July 20
1300
1700
1900
UT, 1981 July 20

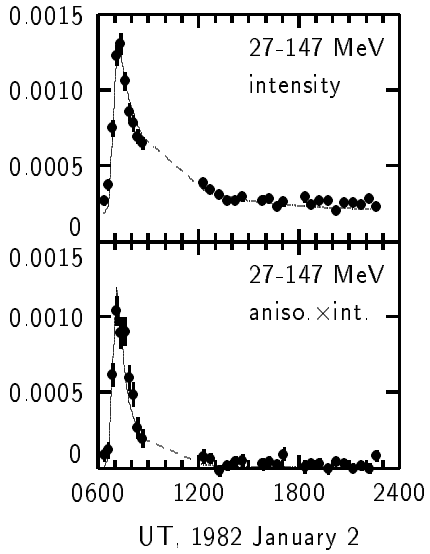
0.0015
0.0010
0.0005
0
27-147 MeV
intensity
0.0015
0.0010
0.0005
0
27-147 MeV
aniso.×int.
0600
1200
1800
2400
UT, 1982 January 2

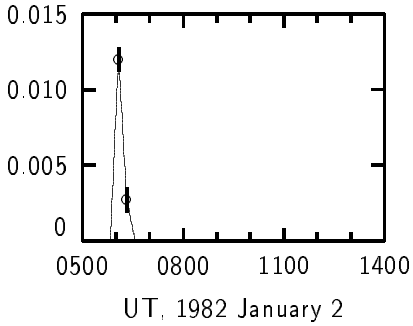
0.015
0.010
0.005
0
0500
0800
1100
1400
UT, 1982 January 2

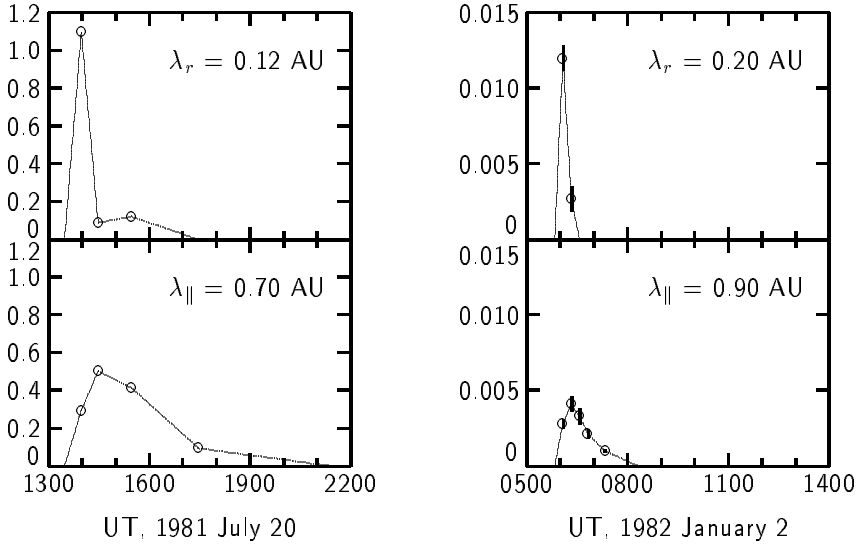
1.2
1.0
0.8
0.6
0.4
0.2
0
λ_r = 0.12 AU
$\lambda_\parallel$ = 0.70 AU
1300
1600
1900
2200
UT, 1981 July 20
0.015
0.010
0.005
0
λ_r = 0.20 AU
$\lambda_\parallel$ = 0.90 AU
0500
0800
1100
1400
UT, 1982 January 2